A Low-Complexity SLM Scheme Using Additive Mapping Sequences for PAPR Reduction of OFDM Signals

Hyun-Bae Jeon, Jong-Seon No, *Senior Member, IEEE*, and Dong-Joon Shin, *Senior Member, IEEE*

***Abstract*—The selected mapping (SLM) scheme is one of the well-known peak-to-average power ratio (PAPR) reduction schemes for orthogonal frequency division multiplexing (OFDM) systems. A number of low-complexity SLM schemes have been proposed but most of them reduce the computational complexity at the cost of bit error rate (BER) or PAPR reduction performance degradation. In this paper, a new low-complexity SLM scheme is proposed, which generates alternative signal sequences by adding mapping signal sequences to an OFDM signal sequence. The proposed scheme considerably reduces the computational complexity without sacrificing BER and PAPR reduction performance only by requiring additional memory to save the additive mapping signal sequences, especially for the OFDM system with quadrature amplitude modulation (QAM). Similarly, a low-complexity SLM scheme is proposed for multi-input multi-output (MIMO) OFDM system with space-frequency block code (SFBC).**

***Index Terms*—Additive mapping sequences, low complexity, orthogonal frequency division multiplexing (OFDM), peak-to-average power ratio (PAPR), selected mapping (SLM).**

I. Introduction

ORTHOGONAL frequency division multiplexing (OFDM) is an attractive technique for wireless communications because it supports robust reliability and high data rate in the frequency selective fading channel environments. However, the OFDM signals show high peak-to-average power ratio (PAPR) in the time domain, which causes significant inter-modulation and undesirable out-of-band radiation when an OFDM signal passes through nonlinear devices such as high power amplifier (HPA) [1], [2].

Several techniques have been proposed to mitigate the high PAPR of OFDM signals [3]. Clipping is used to reduce the peak power by clipping the OFDM signals to the threshold level [4]. Companding scheme scales the time-domain signals nonlinearly such that the signals with large amplitude are suppressed and the signals with small amplitude are expanded [5]–[8]. Tone reservation (TR) [9], tone injection (TI) [9], and active constellation extension (ACE) [10] change constellation points for some subcarriers to reduce the PAPR. Selected mapping (SLM) [11] and partial transmit sequence (PTS) [12] schemes generate several alternative signal sequences representing the same OFDM signal sequence and select the one with the minimum PAPR among them. More alternative signal sequences increase the possibility to improve the PAPR reduction performance, but the computational complexity increases as well.

There are many schemes to reduce the computational complexity of SLM. In [13], inverse discrete Fourier transform (IDFT) to generate alternative signal sequences is replaced by a conversion matrix in the time domain whose elements are composed of $\{0, +1, -1\}$. This scheme reduces the computational complexity significantly but cannot avoid bit error rate (BER) degradation. The low-complexity scheme in [14] modifies discrete Fourier transform (DFT)-shaping SLM scheme such that by using a pre-computed and windowed sparse matrix, a candidate alternative signal sequence with lower PAPR is selected and DFT-shaping scheme is applied only to this sequence. This scheme shows better PAPR reduction as well as lower computational complexity but needs additional memory and computations at the receiver. In [15] and [16], alternative signal sequences are generated at the intermediate stage of fast Fourier transform (FFT) in decimation-in-time [15] or decimation-in-frequency [16]. These schemes have a trade-off between PAPR reduction performance and computational complexity. In [17], through linear combinations of alternative signal sequences, additional alternative signal sequences are generated. Therefore, the computational complexity due to the inverse Fourier transform (IFFT) operations can be reduced while achieving the PAPR reduction performance similar to that of the conventional SLM scheme.

In this paper, a new low-complexity SLM scheme is proposed, which generates alternative signal sequences by adding mapping sequences to an OFDM signal sequence. The proposed scheme considerably reduces the computational complexity without sacrificing BER and PAPR reduction performance. Also, this scheme is extended to the multi-input multi-output (MIMO) OFDM system with space-frequency block coding (SFBC) [20]. Although the proposed scheme is similar to the partial bit inverted SLM (PBISLM) in [21] in the sense that the alternative symbols undergo the change of both amplitude and phase, the proposed scheme seeks to generate the alternative signal sequences with low complexity while the PBISLM is aimed to improve the PAPR reduction performance with

Manuscript received January 09, 2011; revised April 15, 2011; accepted April 22, 2011. Date of publication June 13, 2011; date of current version November 23, 2011. This work was supported by the Korea Science and Engineering Foundation (KOSEF) Grant 2011-0000328 funded by the Korea government (MEST).

H.-B. Jeon and J.-S. No are with the Department of Electrical Engineering and Computer Science, INMC, Seoul National University, Seoul 151-744, Korea (e-mail: lucidream@ccl.snu.ac.kr; jsno@snu.ac.kr).

D.-J. Shin is with the Department of Electronic Engineering, Hanyang University, Seoul 133-791, Korea (e-mail: djshin@hanyang.ac.kr).

Digital Object Identifier 10.1109/TBC.2011.2151570

keeping the computational complexity same as that of the conventional SLM scheme.

The rest of this paper is organized as follows. In Section II, PAPR and some SLM schemes are reviewed. Alternative symbol sequences are expressed by using additive mapping sequences in Section III and a new low-complexity SLM scheme using additive mapping sequences is proposed and evaluated in Section IV. The numerical analysis and conclusions are given in Sections V and VI.

II. Conventional and Partial Bit Inverted SLM Schemes

Assume that a binary input sequence $\mathbf{A}_b = [A_{0,0},\ldots,A_{0,\log_2 M-1},\ldots,A_{N-1,0},\ldots,A_{N-1,\log_2 M-1}]^T$ of length $N\log_2 M$ is modulated into an input symbol sequence $\mathbf{A} = [A_0, A_1,\ldots,A_{N-1}]^T$ of M-ary quadrature amplitude modulation (M-QAM) or M-ary phase shift keying (M-PSK) in OFDM system with N subcarriers. Note that $A_{k,j} \in \{+1,-1\}$ is the jth bit of the kth M-ary symbol. The baseband discrete-time OFDM signal sequence $\mathbf{a} = [a_0, a_1,\ldots,a_{N-1}]^T$ can be written as

$$a_n = \frac{1}{\sqrt{N}}\sum_{k=0}^{N-1} A_k e^{j2\pi nk/N}, \quad 0 \le n < N \tag{1}$$

where n stands for a discrete-time index.

The IDFT expression in (1) can be represented by using an $N \times N$ Hermitian matrix $\mathbf{Q}$ with elements $Q_{k,n} = (1/\sqrt{N})e^{-j2\pi nk/N}$ as

$$\mathbf{a} = \mathbf{Q}^H\mathbf{A} \tag{2}$$

and

$$\mathbf{A} = \mathbf{Q}\mathbf{a}, \tag{3}$$

respectively, where $\mathbf{Q}^H$ denotes the Hermitian of $\mathbf{Q}$.

The PAPR of $\mathbf{a}$ in the discrete-time domain can be defined as

$$\mathrm{PAPR}(\mathbf{a}) \doteq \frac{\max\limits_{0\le n<N} |a_n|^2}{\mathrm{E}\left[|a_n|^2\right]} \tag{4}$$

where $\mathrm{E}[\cdot]$ denotes the expectation operator.

In the conventional SLM scheme, a transmitter generates U distinct alternative signal sequences which represent the same input symbol sequence and selects the one with the minimum PAPR for transmission. By using U different phase sequences of length N, $\mathbf{P}^{(u)} = [P_0^{(u)}, P_1^{(u)},\ldots,P_{N-1}^{(u)}]^T$, $0 \le u < U$, U alternative symbol sequences $\mathbf{X}^{(u)} = [X_0^{(u)}, X_1^{(u)},\ldots,X_{N-1}^{(u)}]^T$, $0 \le u < U$, are generated by $\mathbf{X}^{(u)} = \mathbf{A} \otimes \mathbf{P}^{(u)}$ where $\otimes$ denotes the component-wise multiplication. The first phase sequence $\mathbf{P}^{(0)}$ is usually the all-1 sequence to include an input symbol sequence among alternative symbol sequences. Then, the one with the minimum PAPR among the alternative signal sequences $\mathbf{x}^{(u)} = \mathbf{Q}^H\mathbf{X}^{(u)}$ is finally selected for transmission.

The alternative symbol sequence $\mathbf{X}^{(u)}$ can be rewritten as the binary sequence $\mathbf{X}_b^{(u)} = [X_{0,0}^{(u)},\ldots,X_{0,\log_2 M-1}^{(u)},\ldots,X_{N-1,0}^{(u)},\ldots,X_{N-1,\log_2 M-1}^{(u)}]^T$ of length $N\log_2 M$ and PBISLM in [21] generates $\mathbf{X}_b^{(u)}$ by multiplying some preselected bits of each M-QAM symbol A_k by $P_k^{(u)}$ of a binary phase sequence $\mathbf{P}^{(u)}$. Let $\mathbf{S} = \{i_0, i_1,\ldots,i_{W-1}\} \subset \{0,1,\ldots,\log_2 M-1\}$ denote the index set of the preselected bits among the binary form $\{A_{k,0}, A_{k,1},\ldots,A_{k,\log_2 M-1}\}$ of M-QAM symbol A_k, where W is the number of bits to be multiplied by $P_k^{(u)}$. Then, the jth bit $X_{k,j}^{(u)}$ of the kth symbol in the binary form of the uth alternative symbol sequence $\mathbf{X}_b^{(u)}$ is obtained by

$$X_{k,j}^{(u)} = \begin{cases} A_{k,j}P_k^{(u)}, & j \in \mathbf{S} \\ A_{k,j}, & j \in \mathbf{S}^{\mathrm{C}} \end{cases} \tag{5}$$

where $\mathbf{S}^{\mathrm{C}}$ is the complement set of $\mathbf{S}$ in $\{0,1,\ldots,\log_2 M-1\}$. For example, if $\mathbf{S} = \{0,2\}$ in the binary form $\{A_{k,0}, A_{k,1}, A_{k,2}, A_{k,3}\}$ of 16-QAM symbol A_k, the binary form of $X_k^{(u)}$ becomes $\{-A_{k,0}, A_{k,1}, -A_{k,2}, A_{k,3}\}$ when $P_k^{(u)}$ is -1.

To achieve the best PAPR reduction performance, $\mathbf{S}$ should be selected to minimize the covariance of average symbol powers of the alternative symbol sequences [21]. PBISLM scheme shows better PAPR reduction performance than the conventional SLM scheme because it changes the amplitude as well as the phase of input symbols to generate alternative symbol sequences in OFDM system with M-QAM. More detailed information about PBISLM scheme can be found in [21].

III. Additive Mapping Sequences

Additive mapping sequences are introduced in this section, which will be used in the proposed SLM scheme. In PBISLM scheme for OFDM system with M-QAM, the kth alternative symbol of the uth alternative symbol sequence for the phase sequence $P_k^{(u)} \in \{+1,-1\}$ can be expressed as

$$\begin{aligned} X_k^{(u)} &= A_k + D_k^{(u)} \\ &= \begin{cases} A_k - D(M), & A_k \in \mathcal{Q}^{(1)} \text{ and } P_k^{(u)} = -1 \\ A_k + D(M)^*, & A_k \in \mathcal{Q}^{(2)} \text{ and } P_k^{(u)} = -1 \\ A_k + D(M), & A_k \in \mathcal{Q}^{(3)} \text{ and } P_k^{(u)} = -1 \\ A_k - D(M)^*, & A_k \in \mathcal{Q}^{(4)} \text{ and } P_k^{(u)} = -1 \\ A_k, & P_k^{(u)} = 1 \end{cases} \end{aligned} \tag{6}$$

where $D(M) = d(1+j)\sqrt{M}/2$, $D(M)^*$ denotes the complex conjugate of $D(M)$, d is the smallest distance between M-QAM symbols, and $\mathcal{Q}^{(i)}$ is the set of symbols belonging to the ith quadrant of 2-dimensional signal constellation. Then $\mathbf{D}^{(u)} = [D_0^{(u)}, D_1^{(u)},\ldots,D_{N-1}^{(u)}]^T$, $0 \le u < U$, are called additive mapping sequences. Note that the additive mapping sequences $\mathbf{D}^{(u)}$ are determined by the input symbol sequence $\mathbf{A}$ and the phase sequence $\mathbf{P}^{(u)}$. Fig. 1 shows the alternative symbol mapping for the binary representation of Gray mapped 16-QAM symbols. When $P_k^{(u)} = -1$, the input symbol A_k in 16-QAM constellation is mapped to the symbol with the same shape and color in the opposite quadrant in the PBISLM scheme. Clearly, this symbol mapping can be performed by adding $D_k^{(u)}$ to A_k, when $P_k^{(u)}$ is -1 as given in (6).

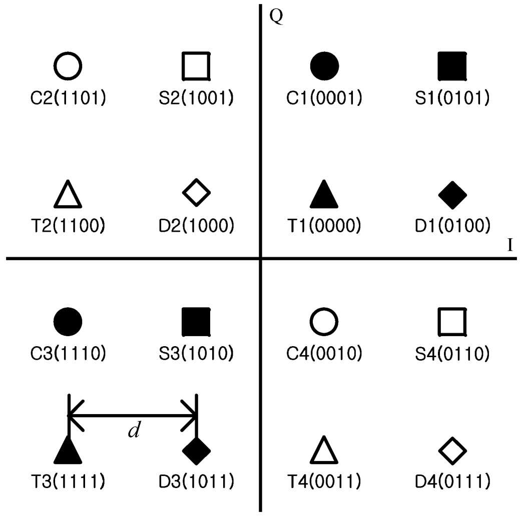

Fig. 1. Alternative symbol mapping for Gray mapped 16-QAM constellation in PBISLM scheme.

Moreover, this additive mapping concept can be extended to generate more alternative symbol sequences by separately considering the in-phase and quadrature components of $D_k^{(u)} = D_{k,I}^{(u)} + jD_{k,Q}^{(u)}$. For example, an input symbol in $\mathcal{Q}^{(1)}$ can be mapped to the symbol with the same shape in $\mathcal{Q}^{(2)}$ by adding the real part $D_{k,I}^{(u)}$ and the symbol with the same shape in $\mathcal{Q}^{(4)}$ by adding the imaginary part $jD_{k,Q}^{(u)}$, respectively. It implies that the symbols with the same shape in Fig. 1 can be the alternative symbols of each other by adding the linear combinations of $D_{k,I}^{(u)}$ and $jD_{k,Q}^{(u)}$.

It should also be noted that for Gray mapped constellation, the $\mathbf{S}$ of indices of bits to be multiplied by the component of phase sequence in PBISLM scheme is partitioned into two subsets, one of bit indices that reflect the change of in-phase components and the other of bit indices that reflect the change of quadrature components. In Fig. 1 where $\mathbf{S} = \{0,1,2,3\}$, two subsets of $\mathbf{S}$ correspond to the sets of indices of two most significant bits (MSBs) and two least significant bits (LSBs), which change in-phase components and quadrature components, respectively. This facilitates SLM decoding at the receiver, which will be explained in the next section.

The kth symbol of the uth alternative symbol sequence in the SLM schemes for OFDM system with M-PSK can also be expressed as

$$X_k^{(u)} = A_k + D_k^{(u)} = \begin{cases} -A_k, & P_k^{(u)} = -1 \\ A_k\,, & P_k^{(u)} = 1. \end{cases} \tag{7}$$

It is clear that this additive representation of alternative symbol sequences changes only the phase of input symbol A_k.

In the next section, a new low-complexity SLM scheme and its decoding scheme are proposed and the computational complexity is evaluated.

IV. New Low-Complexity SLM Scheme

In this section, a new low-complexity SLM scheme is proposed, which uses additive mapping sequences to generate alternative symbol sequences. Also, the computational complexity of the proposed scheme is evaluated and an efficient SLM decoding method is proposed, which reduces the computational complexity without BER degradation.

A. Low-Complexity SLM Scheme for OFDM

Let $\mathbf{P}^{(-1)}$ be the phase sequence whose elements are all -1 and $\mathbf{D}^{(-1)} = \mathbf{D}_I^{(-1)} + j\mathbf{D}_Q^{(-1)}$ be the corresponding additive mapping sequence for the input symbol sequence $\mathbf{A}$, where $\mathbf{D}_I^{(-1)}$ and $\mathbf{D}_Q^{(-1)}$ denote the in-phase and quadrature components of $\mathbf{D}^{(-1)}$, respectively. Note that $\mathbf{D}^{(-1)}$ is determined by the input symbol sequence $\mathbf{A}$ as given in (6) and (7). Then the additive mapping signal sequence $\mathbf{d}^{(-1)}$ is defined as

$$\mathbf{d}^{(-1)} = \mathbf{Q}^H\mathbf{D}^{(-1)} = \mathbf{Q}^H\mathbf{D}_I^{(-1)} + j\mathbf{Q}^H\mathbf{D}_Q^{(-1)}. \tag{8}$$

Let $\mathbf{d}_I^{(-1)} = \mathbf{Q}^H\mathbf{D}_I^{(-1)}$ and $\mathbf{d}_Q^{(-1)} = \mathbf{Q}^H\mathbf{D}_Q^{(-1)}$. Then $\mathbf{d}_I^{(-1)}$ and $\mathbf{d}_Q^{(-1)}$ have the property of complex conjugate symmetry because $\mathbf{D}_I^{(-1)}$ and $\mathbf{D}_Q^{(-1)}$ are real. Similarly, the lth additive mapping signal sequence for $\mathbf{P}_k^{(l)}$ is given as

$$\mathbf{d}^{(l)} = \mathbf{Q}^H\mathbf{D}^{(l)} = \mathbf{Q}^H\mathbf{D}_I^{(l)} + j\mathbf{Q}^H\mathbf{D}_Q^{(l)}, \quad 1 \le l \le V \tag{9}$$

where $\mathbf{d}_I^{(l)} = \mathbf{Q}^H\mathbf{D}_I^{(l)}$ and $\mathbf{d}_Q^{(l)} = \mathbf{Q}^H\mathbf{D}_Q^{(l)}$ also have the property of complex conjugate symmetry because $\mathbf{D}_I^{(l)}$ and $\mathbf{D}_Q^{(l)}$ are also real.

Using the linear combinations of these additive mapping signal sequences $\mathbf{d}_I^{(-1)}$, $j\mathbf{d}_Q^{(-1)}$, $\mathbf{d}_I^{(l)}$, and $j\mathbf{d}_Q^{(l)}$, we can generate 16 different alternative signal sequences as in Table I, where $\mathbf{x}^{(u)} = \mathbf{a} + \mathbf{m}^{(u)}$ and $\mathbf{m}^{(u)}$ is the linear combination of the additive mapping signal sequences $\mathbf{d}_I^{(-1)}$, $j\mathbf{d}_Q^{(-1)}$, $\mathbf{d}_I^{(l)}$, and $j\mathbf{d}_Q^{(l)}$. For example, the row $\mathbf{x}^{(9)}$ denotes $\mathbf{m}^{(u)} = \mathbf{d}_I^{(-1)} - \mathbf{d}_I^{(l)} + j\mathbf{d}_Q^{(l)}$. Generally, adding these additive mapping signal sequences to $\mathbf{a}$ means that input symbol $A_k = A_{k,I} + jA_{k,Q}$ is shifted by $-\mathrm{sgn}(A_{k,I})\sqrt{M}d/2$ only along the real axis, by $-\mathrm{sgn}(A_{k,Q})\sqrt{M}d/2$ only along the imaginary axis, or by these amounts along both axes. In order for $\mathbf{X}^{(u)}$ to take the symbol in the original constellation, subtracting $\mathbf{d}_I^{(l)}$ or $j\mathbf{d}_Q^{(l)}$ from $\mathbf{a}$ should be accompanied by adding $\mathbf{d}_I^{(-1)}$ or $j\mathbf{d}_Q^{(-1)}$, respectively. For example, $\mathbf{x}^{(13)} = \mathbf{a} + \mathbf{m}^{(13)} = \mathbf{a} + \mathbf{d}_I^{(-1)} + j\mathbf{d}_Q^{(-1)} - \mathbf{d}_I^{(l)}$ is the result of $\mathbf{Q}^H\mathbf{X}^{(13)}$, where

$$X_k^{(13)} = \begin{cases} A_k + d\,(-\mathrm{sgn}(A_{I,k}) \\ \qquad -j\mathrm{sgn}(A_{Q,k}))\,\frac{\sqrt{M}}{2}, & P_k^{(l)} = 1 \\ A_k + d\,(-j\mathrm{sgn}(A_{Q,k}))\,\frac{\sqrt{M}}{2}, & P_k^{(l)} = -1. \end{cases} \tag{10}$$

The possible values of the alternative symbol $X_k^{(u)}$ when $A_k =$ T1 in Fig 1 are also listed in the last columns of Table I. It is shown that all possible 16 pairs of four constellation points T1, T2, T3, and T4 with the same shape as A_k are used.

Note that $\mathbf{m}^{(u)}$'s for the first four alternative signal sequences do not include $\mathbf{d}_I^{(l)}$ and $j\mathbf{d}_Q^{(l)}$ and the remaining 12 alternative signal sequences are generated by properly using additional $\mathbf{d}_I^{(l)}$ and $j\mathbf{d}_Q^{(l)}$. Thus, the total number of alternative signal sequences generated from V phase sequences is $4 + 12V$.

TABLE I
ALTERNATIVE SIGNAL SEQUENCES GENERATED BY THE PROPOSED SCHEME (THE TERM MARKED '+' OR '−' IS ADDED TO OR SUBTRACTED FROM $\mathbf{a}$)

u	$\mathbf{x}^{(u)}$	$\mathbf{a}$	$\mathbf{m}^{(u)}$				$X_k^{(u)}$ for A_k=T1 in Fig.1	
			$\mathbf{d}_I^{(-1)}$	$j\mathbf{d}_Q^{(-1)}$	$\mathbf{d}_I^{(l)}$	$j\mathbf{d}_Q^{(l)}$	$P_k^{(l)}=1$	$P_k^{(l)}=-1$
0	$\mathbf{x}^{(0)}$	+					T1	T1
1	$\mathbf{x}^{(1)}$	+	+				T2	T2
2	$\mathbf{x}^{(2)}$	+		+			T4	T4
3	$\mathbf{x}^{(3)}$	+	+	+			T3	T3
4	$\mathbf{x}^{(4)}$	+			+		T1	T2
5	$\mathbf{x}^{(5)}$	+				+	T1	T4
6	$\mathbf{x}^{(6)}$	+			+	+	T1	T3
7	$\mathbf{x}^{(7)}$	+	+		−		T2	T1
8	$\mathbf{x}^{(8)}$	+	+			+	T2	T3
9	$\mathbf{x}^{(9)}$	+	+		−	+	T2	T4
10	$\mathbf{x}^{(10)}$	+		+	+		T4	T3
11	$\mathbf{x}^{(11)}$	+		+		−	T4	T1
12	$\mathbf{x}^{(12)}$	+		+	+	−	T4	T2
13	$\mathbf{x}^{(13)}$	+	+	+	−		T3	T4
14	$\mathbf{x}^{(14)}$	+	+	+		−	T3	T2
15	$\mathbf{x}^{(15)}$	+	+	+	−	−	T3	T1

If the proposed scheme is applied to an OFDM system with M-PSK, the number of alternative signal sequences generated by adding mapping signal sequences is reduced compared to that with M-QAM. An input symbol A_k in 2-dimensional signal constellation can be expressed by $|A_k|e^{j\theta}$, where $|A_k|$ is the magnitude and θ is the angle of A_k. Then the first four alternative signal sequences generated by the proposed scheme for an OFDM system with M-PSK are expressed as

$$\begin{aligned}\mathbf{x}^{(0)} &= \mathbf{a}\\ \mathbf{x}^{(1)} &= \mathbf{a}+\mathbf{d}_I^{(-1)} = \mathbf{a}e^{j(\pi-2\theta)}\\ \mathbf{x}^{(2)} &= \mathbf{a}+j\mathbf{d}_Q^{(-1)} = \mathbf{a}e^{-j2\theta}\\ \mathbf{x}^{(3)} &= \mathbf{a}+\mathbf{d}_I^{(-1)}+j\mathbf{d}_Q^{(-1)} = \mathbf{a}e^{j\pi}.\end{aligned} \tag{11}$$

Since $\mathbf{X}^{(1)}$, $\mathbf{X}^{(2)}$, and $\mathbf{X}^{(3)}$ only change the phase of $\mathbf{a}$, these four alternative signal sequences have the same PAPR. Similarly, the remaining 12 alternative signal sequences for $\mathbf{P}^{(l)}$ in Table I can be partitioned into the following sets with the same PAPR.

$$\begin{aligned}&\left\{\mathbf{a}+\mathbf{d}_I^{(l)}, \mathbf{a}+\mathbf{d}_I^{(-1)}-\mathbf{d}_I^{(l)}, \mathbf{a}+j\mathbf{d}_Q^{(-1)}+\mathbf{d}_I^{(l)}, \mathbf{a}+\mathbf{d}^{(-1)}-\mathbf{d}_I^{(l)}\right\}\\ &\Big\{\mathbf{a}+j\mathbf{d}_Q^{(l)}, \mathbf{a}+j\mathbf{d}_Q^{(-1)}-j\mathbf{d}_Q^{(l)},\\ &\quad \mathbf{a}+\mathbf{d}_I^{(-1)}+j\mathbf{d}_Q^{(l)}, \mathbf{a}+\mathbf{d}^{(-1)}-j\mathbf{d}_Q^{(l)}\Big\}\\ &\Big\{\mathbf{a}+\mathbf{d}^{(l)}, \mathbf{a}+\mathbf{d}_I^{(-1)}-\mathbf{d}_I^{(l)}+j\mathbf{d}_Q^{(l)},\\ &\quad \mathbf{a}+j\mathbf{d}_Q^{(-1)}+\mathbf{d}_I^{(l)}-j\mathbf{d}_Q^{(l)}, \mathbf{a}+\mathbf{d}^{(-1)}-\mathbf{d}^{(I)}\Big\}.\end{aligned} \tag{12}$$

Therefore, by using the proposed scheme for an OFDM system with M-PSK, $1+3V$ alternative signal sequences can be obtained from V phase sequences.

B. Low-Complexity SLM Scheme for MIMO-OFDM

The low-complexity SLM scheme proposed in Section IV-A can be extended to the MIMO-OFDM system. First, the proposed scheme can be applied to the MIMO-OFDM system with space-time block code (STBC) in which each antenna transmits independent OFDM signal sequence during one symbol block period and thus the proposed SLM scheme can be independently used for each antenna. However, in SFBC-OFDM system, data symbols are encoded in the frequency domain and a PAPR reduction scheme applied to one antenna affects the signals from other antennas. Therefore, when a PAPR reduction scheme is used in SFBC-OFDM system, the encoding schemes for all antennas should be considered to keep the orthogonality among them.

In this paper, we consider the Alamouti SFBC-OFDM system [20], where an input symbol sequence $\mathbf{A}$ is encoded to $\mathbf{A}_{SFBC1}$ and $\mathbf{A}_{SFBC2}$ for two transmit antennas as

$$\begin{aligned}\mathbf{A}_{SFBC1} &= \left[A_0, -A_1^*, \ldots, A_{N-2}, -A_{N-1}^*\right]^T\\ \mathbf{A}_{SFBC2} &= \left[A_1, A_0^*, \ldots, A_{N-1}, A_{N-2}^*\right]^T.\end{aligned} \tag{13}$$

$\mathbf{A}_{SFBC1}$ can be divided into even and odd subcarrier indices as $\mathbf{A}_{SFBC1} = \mathbf{A}_{SFBC1,e} + \mathbf{A}_{SFBC1,o}$, where

$$\begin{aligned}\mathbf{A}_{SFBC1,e} &= [A_0, 0, A_2, 0, \ldots, A_{N-2}, 0]^T\\ \mathbf{A}_{SFBC1,o} &= \left[0, -A_1^*, 0, -A_3^* \ldots, 0, -A_{N-1}^*\right]^T.\end{aligned} \tag{14}$$

$\mathbf{A}_{SFBC2}$ can be similarly divided into even and odd subcarrier indices as $\mathbf{A}_{SFBC2} = \mathbf{A}_{SFBC2,e} + \mathbf{A}_{SFBC2,o}$. Clearly, $\mathbf{A}_{SFBC2,e}$ and $\mathbf{A}_{SFBC2,o}$ can be obtained by linearly transforming $\mathbf{A}^*_{SFBC1,o}$ and $\mathbf{A}^*_{SFBC1,e}$, respectively, as

$$\begin{aligned}\mathbf{A}_{SFBC2,e} &= -\mathbf{C}_{-1}\mathbf{A}^*_{SFBC1,o}\\ \mathbf{A}_{SFBC2,o} &= \mathbf{C}_1\mathbf{A}^*_{SFBC1,e}\end{aligned} \tag{15}$$

where $\mathbf{C}_{-1}$ and $\mathbf{C}_1$ are $N \times N$ matrices which cyclically shift a vector by one position upward and downward, respectively.

In the conventional SLM scheme for the Alamouti SFBC-OFDM, the uth alternative signal sequence $\mathbf{x}_{SFBC1}^{(u)}$ of $\mathbf{A}_{SFBC1}$ is generated in the same way as the single-antenna OFDM case as

$$\mathbf{x}_{SFBC1}^{(u)} = \mathbf{Q}^H\mathbf{X}_{SFBC1}^{(u)} = \mathbf{Q}^H(\mathbf{A}_{SFBC1} \otimes \mathbf{P}^{(u)}). \tag{16}$$

Then the uth alternative signal sequence $\mathbf{x}_{SFBC2}^{(u)}$ of $\mathbf{A}_{SFBC2}$ is obtained by using $\mathbf{X}_{SFBC1}^{(u)}$ as

$$\begin{aligned}\mathbf{x}_{SFBC2}^{(u)} &= \mathbf{Q}^H\mathbf{X}_{SFBC2}^{(u)}\\ &= \mathbf{Q}^H\left(-\mathbf{C}_{-1}\mathbf{X}^*_{SFBC1,o} + \mathbf{C}_1\mathbf{X}^*_{SFBC1,e}\right).\end{aligned} \tag{17}$$

Finally, $\mathbf{x}_{SFBC1}^{(\tilde{u})}$ and $\mathbf{x}_{SFBC2}^{(\tilde{u})}$ are selected for transmission by the following criterion

$$\tilde{u} = \arg\min_{0\le u<U} \max\left\{\mathrm{PAPR}\left(\mathbf{x}_{SFBC1}^{(u)}\right), \mathrm{PAPR}\left(\mathbf{x}_{SFBC2}^{(u)}\right)\right\}. \tag{18}$$

To apply the proposed SLM scheme to the Alamouti SFBC-OFDM system, the additive mapping signal sequence $\mathbf{d}_{SFBC1}^{(-1)}$ corresponding to $\mathbf{P}^{(-1)}$ and the additive mapping signal sequence $\mathbf{d}_{SFBC1}^{(l)}$ corresponding to $\mathbf{P}^{(l)}$ for $\mathbf{A}_{SFBC1}$ are also divided into even and odd terms as (14) and each term is further divided into in-phase and quadrature components as (8) and (9) for the single-antenna OFDM case as follows.

$$\begin{aligned}\mathbf{d}_{SFBC1}^{(-1)} &= \mathbf{Q}^H\mathbf{D}_{SFBC1}^{(-1)}\\ &= \mathbf{Q}^H\left(\mathbf{D}_{e,I}^{(-1)} + j\mathbf{D}_{e,Q}^{(-1)} + \mathbf{D}_{o,I}^{(-1)} + j\mathbf{D}_{o,Q}^{(-1)}\right)\end{aligned} \tag{19}$$

and

$$\mathbf{d}_{SFBC1}^{(l)} = \mathbf{Q}^H \mathbf{D}_{SFBC1}^{(l)} = \mathbf{Q}^H \left(\mathbf{D}_{e,I}^{(l)} + j\mathbf{D}_{e,Q}^{(l)} + \mathbf{D}_{o,I}^{(l)} + j\mathbf{D}_{o,Q}^{(l)}\right) \quad (20)$$

where $\mathbf{D}_{e,I}^{(-1)}$, $\mathbf{D}_{e,Q}^{(-1)}$, $\mathbf{D}_{o,I}^{(-1)}$, and $\mathbf{D}_{o,Q}^{(-1)}$ are in-phase and quadrature components of even terms and in-phase and quadrature components of odd terms for $\mathbf{D}_{SFBC1}^{(-1)}$, respectively. Similar notations can be used for $\mathbf{D}_{SFBC1}^{(l)}$.

As in (15), the even and odd terms of the lth additive mapping sequence for $\mathbf{A}_{SFBC2}$ can be represented by the linear transforms of $\mathbf{D}_{SFBC1,o}^{*}$ and $\mathbf{D}_{SFBC1,e}^{*}$, respectively, as

$$\mathbf{D}_{SFBC2,e}^{(l)} = -\mathbf{C}_{-1}\mathbf{D}_{SFBC1,o}^{(l)*} = \mathbf{C}_{-1}\left(-\mathbf{D}_{o,I}^{(l)} + j\mathbf{D}_{o,Q}^{(l)}\right)$$
$$\mathbf{D}_{SFBC2,o}^{(l)} = \mathbf{C}_{1}\mathbf{D}_{SFBC1,e}^{(l)*} = \mathbf{C}_{1}\left(\mathbf{D}_{e,I}^{(l)} - j\mathbf{D}_{e,Q}^{(l)}\right). \quad (21)$$

Therefore, the additive mapping sequence for $\mathbf{A}_{SFBC2}$ becomes

$$\mathbf{D}_{SFBC2}^{(l)} = \left(\mathbf{C}_1\mathbf{D}_{e,I}^{(l)} - \mathbf{C}_{-1}\mathbf{D}_{o,I}^{(l)}\right) - j\left(\mathbf{C}_1\mathbf{D}_{e,Q}^{(l)} - \mathbf{C}_{-1}\mathbf{D}_{o,Q}^{(l)}\right). \quad (22)$$

Note that $\mathbf{C}_1\mathbf{D}_{e,I}^{(l)}$, $-\mathbf{C}_1\mathbf{D}_{e,Q}^{(l)}$, $-\mathbf{C}_{-1}\mathbf{D}_{o,I}^{(l)}$, and $\mathbf{C}_{-1}\mathbf{D}_{o,Q}^{(l)}$ are in-phase and quadrature components of odd terms and in-phase and quadrature components of even terms for $\mathbf{D}_{SFBC2}^{(l)}$, respectively.

Let $\mathbf{c}_k = [1, e^{j2\pi k/N}, e^{j2\pi(2k)/N}, \ldots, e^{j2\pi(N-1)k/N}]^T$, $\mathbf{d}_{e,I}^{(l)} = \mathbf{Q}^H\mathbf{D}_{e,I}^{(l)}$, $\mathbf{d}_{e,Q}^{(l)} = \mathbf{Q}^H\mathbf{D}_{e,Q}^{(l)}$, $\mathbf{d}_{o,I}^{(l)} = \mathbf{Q}^H\mathbf{D}_{o,I}^{(l)}$, and $\mathbf{d}_{o,Q}^{(l)} = \mathbf{Q}^H\mathbf{D}_{o,Q}^{(l)}$. Since the additive mapping signal sequence $\mathbf{d}_{SFBC2}^{(l)}$ for $\mathbf{A}_{SFBC2}$ is related to $\mathbf{d}_{SFBC1}^{(l)}$ through (22), $\mathbf{d}_{SFBC2}^{(l)}$ can be obtained as

$$\begin{aligned}\mathbf{d}_{SFBC2}^{(l)} &= \mathbf{Q}^H\mathbf{D}_{SFBC2}^{(l)} \\ &= \left(\mathbf{c}_1 \otimes \mathbf{d}_{e,I}^{(l)} - \mathbf{c}_{-1} \otimes \mathbf{d}_{o,I}^{(l)}\right) \\ &\quad - j\left(\mathbf{c}_1 \otimes \mathbf{d}_{e,Q}^{(l)} - \mathbf{c}_{-1} \otimes \mathbf{d}_{o,Q}^{(l)}\right) \\ &= \Phi\left(\mathbf{d}_I^{(l)}\right) - j\Phi\left(\mathbf{d}_Q^{(l)}\right) \end{aligned} \quad (23)$$

where $\Phi(\mathbf{d}_I^{(l)}) = \mathbf{c}_1 \otimes \mathbf{d}_{e,I}^{(l)} - \mathbf{c}_{-1} \otimes \mathbf{d}_{o,I}^{(l)}$ and $\Phi(\mathbf{d}_Q^{(l)}) = \mathbf{c}_1 \otimes \mathbf{d}_{e,Q}^{(l)} - \mathbf{c}_{-1} \otimes \mathbf{d}_{o,Q}^{(l)}$. It is known that $\Phi(\mathbf{d}_I^{(l)})$ and $\Phi(\mathbf{d}_Q^{(l)})$ can be obtained only by sign inversions, complex conjugations, reordering of $\mathbf{d}_{e,I}^{(l)}$, $\mathbf{d}_{o,I}^{(l)}$, $\mathbf{d}_{e,Q}^{(l)}$, and $\mathbf{d}_{o,Q}^{(l)}$, followed by additional $N/2$ complex multiplication and N complex addition [25]. Similarly, when the additive mapping signal sequence for $\mathbf{A}_{SFBC1}$ and $\mathbf{P}^{(-1)}$ is $\mathbf{d}_{SFBC1}^{(-1)}$, the additive mapping signal sequence $\mathbf{d}_{SFBC2}^{(-1)}$ for $\mathbf{A}_{SFBC2}$ becomes

$$\begin{aligned}\mathbf{d}_{SFBC2}^{(-1)} &= \mathbf{Q}^H\mathbf{D}_{SFBC2}^{(-1)} \\ &= \left(\mathbf{c}_1 \otimes \mathbf{d}_{e,I}^{(-1)} - \mathbf{c}_{-1} \otimes \mathbf{d}_{o,I}^{(-1)}\right) \\ &\quad - j\left(\mathbf{c}_1 \otimes \mathbf{d}_{e,Q}^{(-1)} - \mathbf{c}_{-1} \otimes \mathbf{d}_{o,Q}^{(-1)}\right) \\ &= \Phi\left(\mathbf{d}_I^{(-1)}\right) - j\Phi\left(\mathbf{d}_Q^{(-1)}\right). \end{aligned} \quad (24)$$

Once the alternative signal sequences for $\mathbf{A}_{SFBC1}$ are generated by the same way for the single-antenna case as in Table I, the alternative signal sequences for $\mathbf{A}_{SFBC2}$ can be easily determined by (23) and (24). For example, if $\mathbf{x}_{SFBC1}^{(12)} = \mathbf{a}_{SFBC1} + \mathbf{m}^{(12)} = \mathbf{a}_{SFBC1} + j\mathbf{d}_Q^{(-1)} + \mathbf{d}_I^{(l)} - j\mathbf{d}_Q^{(l)}$, then $\mathbf{x}_{SFBC2}^{(12)} = \mathbf{a}_{SFBC2} - j\Phi(\mathbf{d}_Q^{(-1)}) + \Phi(\mathbf{d}_I^{(l)}) + j\Phi(\mathbf{d}_Q^{(l)})$.

Therefore, the total number of alternative signal sequences generated from V phase sequences for the Alamouti SFBC-OFDM is $4 + 12V$ and $1 + 3V$ for M-QAM and M-PSK, respectively.

C. Computational Complexity of the Proposed SLM Schemes

It is known that the computational complexity of two real N-point IFFTs is equivalent to that of one complex N-point IFFT and $N-2$ complex additions ($2N-4$ real additions) [22]. In the proposed SLM scheme, one complex IFFT for an input symbol sequence $\mathbf{A}$ and two real IFFTs for $\mathbf{D}_I^{(-1)}$ and $\mathbf{D}_Q^{(-1)}$ are needed to generate the first four alternative signal sequences, and two real IFFTs for $\mathbf{D}_I^{(l)}$ and $\mathbf{D}_Q^{(l)}$ are needed to generate the additional 12 alternative signal sequences as in Table I.

We only consider the computational complexity to generate alternative signal sequences for comparison because the remaining computational complexity is the same for most SLM schemes if the number of alternative signal sequences is the same. Table II compares the computational complexity of the conventional and the proposed SLM schemes for single-antenna OFDM and Alamouti SFBC-OFDM systems, where U is the total number of alternative signal sequences and J is the oversampling factor. It is assumed that the computational complexity of two real additions is equivalent to that of one complex addition, and the number of complex multiplications and additions of the JN-point IFFT are $(JN/2)\log_2(JN)$ and $JN\log_2(JN)$, respectively.

For the proposed SLM scheme with M-QAM, two complex IFFTs and $JN-2$ complex additions are needed to generate $\mathbf{a}$, $\mathbf{d}_I^{(-1)}$, and $\mathbf{d}_Q^{(-1)}$, and V complex IFFTs and $V(JN-2)$ complex additions are required to generate V $\mathbf{d}_I^{(l)}$'s and V $\mathbf{d}_Q^{(l)}$'s, where $V = \lceil (U-4)/12 \rceil$ and $\lceil x \rceil$ is the smallest integer not less than x. Also, alternative signal sequences can be generated with $3JN$ complex additions for $\mathbf{x}^{(0)}$ to $\mathbf{x}^{(3)}$ and $12JN$ complex additions for the remaining 12 alternative signal sequences for each l, $1 \le l \le V$, with careful ordering, for example, the order of $\mathbf{x}^{(0)}, \mathbf{x}^{(1)}, \mathbf{x}^{(3)}, \mathbf{x}^{(2)}$, and the order of $\mathbf{x}^{(5)}, \mathbf{x}^{(6)}, \mathbf{x}^{(4)}, \mathbf{x}^{(10)}, \mathbf{x}^{(12)}, \mathbf{x}^{(11)}, \mathbf{x}^{(14)}, \mathbf{x}^{(15)}, \mathbf{x}^{(13)}, \mathbf{x}^{(7)}, \mathbf{x}^{(9)}, \mathbf{x}^{(8)}$ in Table I. Therefore, to generate U alternative signal sequences for OFDM system with M-QAM by the proposed SLM scheme, the total number of required complex multiplications is

$$2\frac{JN}{2}\log_2(JN) + V\frac{JN}{2}\log_2(JN) = \left(2 + \left\lceil \frac{U-4}{12} \right\rceil\right)\frac{JN}{2}\log_2(JN) \quad (25)$$

and the total number of required complex additions is

$$\begin{aligned}&2JN\log_2(JN) + VJN\log_2(JN) \\ &\quad + (V+1)(JN-2) + (12V+3)JN \\ &\quad = \left(2 + \left\lceil \frac{U-4}{12} \right\rceil\right) JN\log_2(JN) \\ &\qquad + \left(13\left\lceil \frac{13U-4}{12} \right\rceil + 4\right) JN - 2\left(\left\lceil \frac{U-4}{12} \right\rceil + 1\right). \end{aligned} \quad (26)$$

TABLE II
COMPUTATIONAL COMPLEXITY OF THE CONVENTIONAL SLM, THE LOW-COMPLEXITY SLM IN [16] AND [17], AND THE PROPOSED SLM SCHEMES. $S = \log_2(JN)$ AND $S - v$ IS THE NUMBER OF THE REMAINING STAGES IN [16]

	Total number of complex multiplications	Total number of complex additions
Conventional SLM	$\frac{U}{2}JN\log_2(JN)$	$UJN\log_2(JN)$
SLM in [16]	$\sum_{b=1}^{v-1} 2^{b-1}\left(\frac{JN}{2^b}-1\right) + U\sum_{b=v}^{S} 2^{b-1}\left(\frac{JN}{2^b}-1\right)$	$JN\left[v + U(S-v)\right]$
SLM in [17]	$\frac{\sqrt{U}JN}{2}\log_2(JN) + JN\left(U-\sqrt{U}\right)$	$\sqrt{U}JN\log_2(JN) + JN(U-\sqrt{U})$
Proposed SLM with M-QAM	$\left(2+\lceil\frac{U-4}{12}\rceil\right)\frac{JN}{2}\log_2(JN)$	$\left(2+\lceil\frac{U-4}{12}\rceil\right)JN\log_2(JN) + \left(13\lceil\frac{13U-4}{12}\rceil+4\right)JN - 2\left(\lceil\frac{U-4}{12}\rceil+1\right)$
Proposed SLM with M-PSK	$\left(1+\lceil\frac{U-1}{3}\rceil\right)\frac{JN}{2}\log_2(JN)$	$\left(1+\lceil\frac{U-1}{3}\rceil\right)JN\log_2(JN) + 4\lceil\frac{U-1}{3}\rceil JN - 2\lceil\frac{U-1}{3}\rceil$
Conventional SLM (SFBC)	$\frac{U}{2}JN\log_2(JN) + \frac{U}{2}JN$	$UJN\log_2(JN) + UJN$
Proposed SLM with M-QAM (SFBC)	$\left(2+\lceil\frac{U-4}{12}\rceil\right)\frac{JN}{2}(\log_2(JN)+1)$	$\left(2+\lceil\frac{U-4}{12}\rceil\right)JN\log_2(JN) + \left(9+26\lceil\frac{U-4}{12}\rceil\right)JN - 2\left(1+\lceil\frac{U-4}{12}\rceil\right)$
Proposed SLM with M-PSK (SFBC)	$\left(1+\lceil\frac{U-1}{3}\rceil\right)\frac{JN}{2}(\log_2(JN)+1)$	$\left(1+\lceil\frac{U-1}{3}\rceil\right)JN\log_2(JN) + \left(1+8\lceil\frac{U-1}{3}\rceil\right)JN - 2\lceil\frac{U-1}{3}\rceil$

Similarly, to generate U alternative signal sequences for OFDM system with M-PSK by the proposed SLM scheme, the total number of required complex multiplications is

$$\frac{JN}{2}\log_2(JN) + V\frac{JN}{2}\log_2(JN) = \left(1+\left\lceil\frac{U-1}{3}\right\rceil\right)\frac{JN}{2}\log_2(JN) \quad (27)$$

and the total number of required complex additions is

$$\begin{aligned} &JN\log_2(JN) + VJN\log_2(JN) + V(JN-2) + 3VJN \\ &= \left(1+\left\lceil\frac{U-1}{3}\right\rceil\right)JN\log_2(JN) \\ &\quad + 4\left\lceil\frac{U-1}{3}\right\rceil JN - 2\left\lceil\frac{U-1}{3}\right\rceil \end{aligned} \quad (28)$$

where $V = \lceil(U-1)/3\rceil$.

By applying the conventional SLM scheme to the Alamouti SFBC-OFDM, $\mathbf{x}_{SFBC2}^{(u)}$ can be generated using sign inversions, complex conjugations, and reordering of even and odd terms of $\mathbf{x}_{SFBC1}^{(u)}$ followed by the additional $JN/2$ complex multiplications and JN complex additions [25]. Therefore, the total number of required complex multiplications and complex additions are $(U/2)JN\log_2(JN) + (U/2)JN$ and $UJN\log_2(JN) + UJN$, respectively.

If the proposed SLM scheme is used for the Alamouti SFBC-OFDM, $\Phi(\mathbf{d}_I^{(l)})$ and $\Phi(\mathbf{d}_Q^{(l)})$ in (23) and $\Phi(\mathbf{d}_I^{(-1)})$ and $\Phi(\mathbf{d}_Q^{(-1)})$ in (24) are also calculated with the additional $JN/2$ complex multiplications and JN complex additions. To generate alternative signal sequences $\mathbf{x}_{SFBC2}^{(0)}$ to $\mathbf{x}_{SFBC2}^{(15)}$, $3JN$ complex additions for $\mathbf{x}_{SFBC2}^{(0)}$ to $\mathbf{x}_{SFBC2}^{(3)}$ and $12JN$ complex additions for the remaining 12 alternative signal sequences for each l, $1 \le l \le V$, are also required. Therefore, to generate U alternative signal sequences for the Alamouti SFBC-OFDM with M-QAM by using the proposed SLM scheme, the total number of required complex multiplications is

$$2\frac{JN}{2}\log_2(JN) + V\frac{JN}{2}\log_2(JN) + 2\frac{JN}{2} + V\frac{JN}{2} = \left(2+\left\lceil\frac{U-4}{12}\right\rceil\right)\frac{JN}{2}(\log_2(JN)+1) \quad (29)$$

and the total number of required complex additions is

$$\begin{aligned} &2JN\log_2(JN) + VJN\log_2(JN) + (V+1)(JN-2) \\ &\quad + (12V+3)JN + (2+V)JN + (12V+3)JN \\ &= \left(2+\left\lceil\frac{U-4}{12}\right\rceil\right)JN\log_2(JN) \\ &\quad + \left(9+26\left\lceil\frac{U-4}{12}\right\rceil\right)JN - 2\left(1+\left\lceil\frac{U-4}{12}\right\rceil\right). \end{aligned} \quad (30)$$

Similarly, to generate U alternative signal sequences for the Alamouti SFBC-OFDM with M-PSK by using the proposed SLM scheme, the total number of required complex multiplications is

$$\frac{JN}{2}\log_2(JN) + V\frac{JN}{2}\log_2(JN) + \frac{JN}{2} + V\frac{JN}{2} = \left(1+\left\lceil\frac{U-1}{3}\right\rceil\right)\frac{JN}{2}(\log_2(JN)+1) \quad (31)$$

and the total number of required complex additions is

$$\begin{aligned} &JN\log_2(JN) + VJN\log_2(JN) + V(JN-2) \\ &\quad + 3VJN + (1+V)JN + 3VJN \\ &= \left(1+\left\lceil\frac{U-1}{3}\right\rceil\right)JN\log_2(JN) \\ &\quad + \left(1+8\left\lceil\frac{U-1}{3}\right\rceil\right)JN - 2\left\lceil\frac{U-1}{3}\right\rceil. \end{aligned} \quad (32)$$

Fig. 2 compares the computational complexity of the conventional SLM, SLM in [16], SLM in [17], and the proposed SLM scheme for $N = 512$ and $J = 4$. Although many low-complexity SLM schemes have been proposed as mentioned in Section I, the proposed scheme is compared with the schemes in [16] and [17] because their PAPR reduction performance is similar to that of the proposed scheme and they have no BER degradation, transmission power increment, and the additional complexity at the receiver. For QPSK, $U = 4$, 7, 10, and 13 are considered and for 16-QAM, $U = 16$, 28, 40, and 52 are considered for the proposed scheme. Note that the modulation

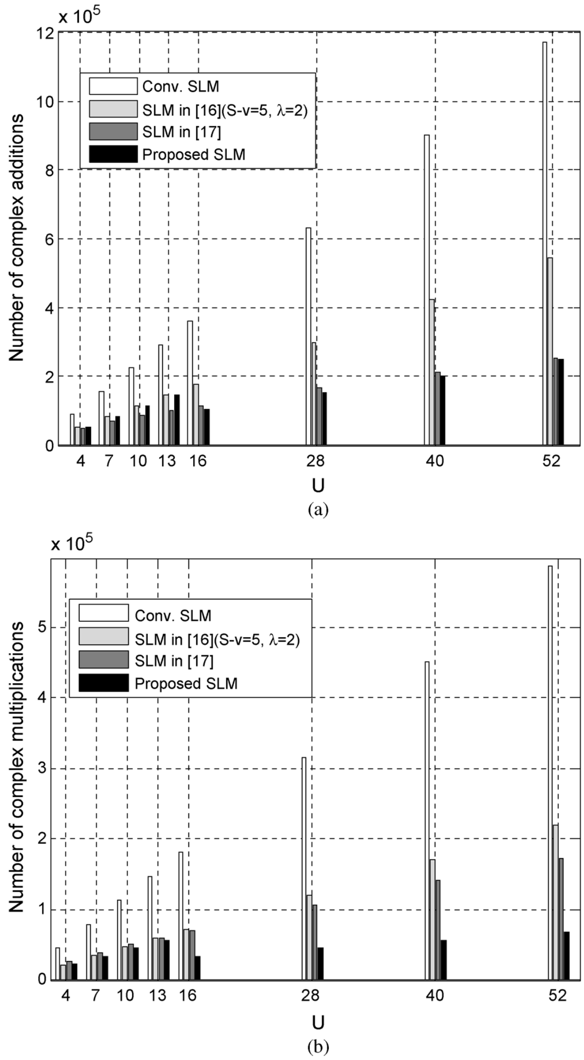

Fig. 2. Comparison of the computational complexity of the conventional SLM, existing low-complexity SLM, and the proposed SLM schemes for $N = 512$ and $J = 4$ ($U = 4$, 7, 10, and 13 for QPSK, and $U = 16$, 28, 40, and 52 for 16-QAM are considered for the proposed scheme. The modulation type does not matter for other schemes.). (a) The number of complex additions. (b) The number of complex multiplications.

type does not affect the complexity of other schemes. The proposed SLM scheme reduces the complexity more for M-QAM and complex multiplication than for M-PSK and complex addition, which is desirable because M-QAM is usually preferred to M-PSK and the complexity of complex multiplication is higher than that of complex addition.

Note that the additional memory of length $JN/2$ is required to save the additive mapping signal sequences $\mathbf{d}_I^{(-1)}$, $\mathbf{d}_Q^{(-1)}$, $\mathbf{d}_I^{(l)}$, and $\mathbf{d}_Q^{(l)}$, respectively, in the proposed SLM scheme. Also, the memory of length JN for each of $\Phi(\mathbf{d}_I^{(-1)})$, $\Phi(\mathbf{d}_Q^{(-1)})$, $\Phi(\mathbf{d}_I^{(l)})$, and $\Phi(\mathbf{d}_Q^{(l)})$ is additionally required for the Alamouti SFBC-OFDM in the proposed SLM scheme. However, this additional memory does not depend on the number of alternative signal sequences U and only the memory to save $2JN$ complex numbers for the single-antenna OFDM and the memory to save $6JN$ complex numbers for the Alamouti SFBC-MIMO are required.

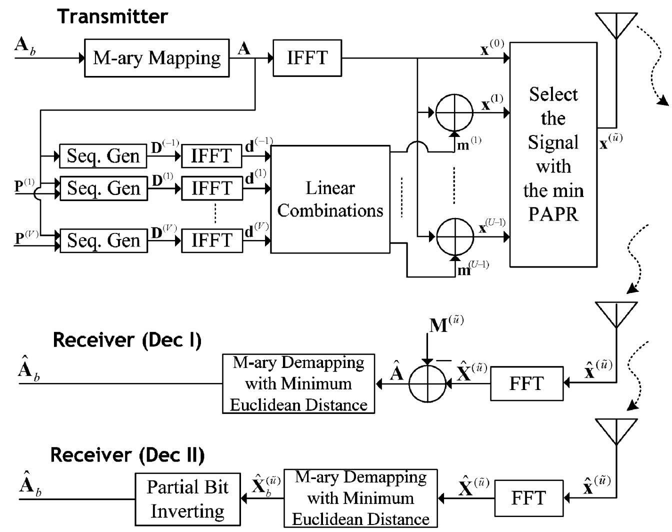

Fig. 3. Block diagram of a transmitter and two receivers for the proposed SLM scheme.

D. Efficient Decoding for the Proposed SLM Scheme

For decoding, it is assumed that the receiver recovers the perfect side information. There are two decoding methods for the proposed SLM scheme at the receiver. The first one denoted as Dec I is to subtract the additive mapping sequence from the received OFDM symbol. Let $\hat{\mathbf{x}}^{(\tilde{u})}$ and $\hat{\mathbf{X}}^{(\tilde{u})} = \mathbf{Q}\hat{\mathbf{x}}^{(\tilde{u})}$ be the received signal sequence and the received symbol sequence at the receiver, respectively. Then the estimated input symbol sequence $\hat{\mathbf{A}}$ is given as

$$\hat{\mathbf{A}} = \hat{\mathbf{X}}^{(\tilde{u})} - \mathbf{M}^{(\tilde{u})} \tag{33}$$

where $\mathbf{M}^{(\tilde{u})} = \mathbf{Q}\mathbf{m}^{(\tilde{u})} = [M_0^{(\tilde{u})}, M_1^{(\tilde{u})}, \ldots, M_{N-1}^{(\tilde{u})}]^T$ is a linear combination of additive mapping sequences determined by the side information $\tilde{u}$. Finally, the symbol sequence in (33) is demapped into the binary sequence $\hat{\mathbf{A}}_b$.

In the second decoding method denoted by Dec II, $\hat{\mathbf{X}}^{(\tilde{u})}$ is firstly evaluated by hard decision and then $\hat{\mathbf{A}}_b$ is obtained through the operation in (33) and demapping. Note that the operation in (33) for Dec II can be replaced by binary operation called partial bit inverting as in PBISLM if the input symbol sequence is modulated with Gray mapping. That is, $\hat{\mathbf{X}}^{(\tilde{u})}$ is demapped into the binary sequence $\hat{\mathbf{X}}_b^{(\tilde{u})}$ and it is decoded into $\hat{\mathbf{A}}_b$ by inverting the bits selected from the side information $\tilde{u}$. For example, the partial bit inverting for $X_k = A_k + D_{k,I}^{(-1)}$ is equivalent to inverting two MSBs of A_k and the partial bit inverting $X_k = A_k + jD_{k,Q}^{(-1)}$ is equivalent to inverting two LSBs of A_k in Fig. 1. Therefore, the receiver complexity to obtain $\hat{\mathbf{A}}$ from $\hat{\mathbf{X}}^{(\tilde{u})}$ in Dec II is negligible. Fig. 3 shows the block diagrams of a transmitter and two receivers using Dec I and Dec II for the proposed SLM scheme.

It will be shown that the BER performance of Dec II is a little bit better than that of Dec I from numerical results in the next section, which can be intuitively inferred from the following example. Assume that $A_k = \mathrm{S3} = -0.5d - j0.5d$ and $M_k^{(\tilde{u})} = 2d + j2d$, which results in $X_k^{(\tilde{u})} = \mathrm{S1} = 1.5d + j1.5d$ in Fig. 1. Then the decision boundary of the received symbol $\hat{X}_k^{(\tilde{u})}$ by Dec

TABLE III
COMPUTATIONAL COMPLEXITY REDUCTION RATIO OF THE PROPOSED SLM SCHEME OVER THE CONVENTIONAL SLM SCHEME FOR $N = 512$ AND $J = 4$

	single-antenna OFDM						Alamouti SFBC-OFDM					
	M-QAM			M-PSK			M-QAM			M-PSK		
U	16	28	40	4	7	10	16	28	40	4	7	10
CCRR for complex multiplication (%)	81	86	88	50	57	60	81	86	88	50	57	60
CCRR for complex addition (%)	72	76	78	41	47	49	65	69	70	35	40	42

TABLE IV
COMPUTATIONAL COMPLEXITY REDUCTION RATIO OF THE PROPOSED SLM SCHEME OVER THE CONVENTIONAL SLM SCHEME FOR $N = 512$ AND $J = 4$

	single-antenna OFDM						Alamouti SFBC-OFDM					
	M-QAM			M-PSK			M-QAM			M-PSK		
A_{th}(dB)	7.8	8.2	8.6	8.2	8.6	9.0	8.0	8.4	8.8	8.4	8.8	9.2
CCRR for complex multiplication (%)	87	64	22	63	50	34	81	69	27	33	32	19
CCRR for complex addition (%)	80	57	7	55	46	33	54	57	5	3	13	7

I is $d < \hat{X}_{k,I}^{(\tilde{u})}, \hat{X}_{k,Q}^{(\tilde{u})} \leq 2d$ since $\hat{A}_k = \hat{X}_k^{(\tilde{u})} - M_k^{(\tilde{u})}$. On the other hand, the decision boundary of $\hat{X}_k^{(\tilde{u})}$ by Dec II is $\hat{X}_{k,I}^{(\tilde{u})}$, $\hat{X}_{k,Q}^{(\tilde{u})} > d$, which is the same as that of the original OFDM symbol. In another case such that $A_k = \mathrm{S1} = 1.5d + j1.5d$ and $X_k^{(\tilde{u})} = \mathrm{S3} = -0.5d - j0.5d$, $-d < \hat{X}_{k,I}^{(\tilde{u})}$, $\hat{X}_{k,Q}^{(\tilde{u})} \leq 0$ is the common decision boundary for Dec I and Dec II and $\hat{X}_{k,I}^{(\tilde{u})}$, $\hat{X}_{k,Q}^{(\tilde{u})} > d$ is added for the decision boundary of Dec I. Since the decision boundary of Dec II in the first case is larger than that of Dec I in the second case, the BER performance of Dec II is slightly better than that of Dec I.

Consequently, the decision boundary of the received symbol for Dec II is the same as that of the original OFDM symbol and therefore the same BER performance is obtained. However, the decision boundary of the received symbol for Dec I is different from that of the original OFDM symbol, which results in the worse BER performance than the original OFDM symbol as in Fig. 6.

V. NUMERICAL ANALYSIS

In this section, the PAPR reduction performance of the conventional SLM and the proposed SLM schemes are compared. The rows of cyclic Hadamard matrix are used as phase sequences [23] and the oversampling factor J is set to 4.

Table III shows the computational complexity reduction ratio (CCRR) of the proposed SLM scheme over the conventional SLM scheme defined as

$$\mathrm{CCRR} = \left(1 - \frac{\text{Complexity of the proposed SLM}}{\text{Complexity of the conventional SLM}}\right) \times 100(\%). \tag{34}$$

CCRR increases as U increases and CCRR for M-QAM and complex multiplication is higher than that for M-PSK and complex addition, respectively.

Also, Table IV lists the CCRR when the conventional and the proposed SLM schemes are simulated by increasing U until the minimum PAPR becomes under the threshold level A_{th} for fair comparison. Note that the proposed scheme is more computationally effective as A_{th} decreases, that is, more rigid PAPR reduction performance is required.

Fig. 4 shows the complementary cumulative distribution functions (CCDFs) of various SLM schemes for QPSK and 16-QAM with $N = 512$. The PAPR reduction performance of the proposed SLM scheme is slightly worse than that of the conventional SLM scheme for QPSK. It is because the alternative symbol sequences of the proposed SLM scheme do not satisfy the optimal conditions for the phase sequences in [23], [24] even if the phase sequences $\mathbf{P}_k^{(l)}$ meet these optimal conditions. However, the performance degradation is within 0.1 dB, which is negligible for the reduced computational complexity.

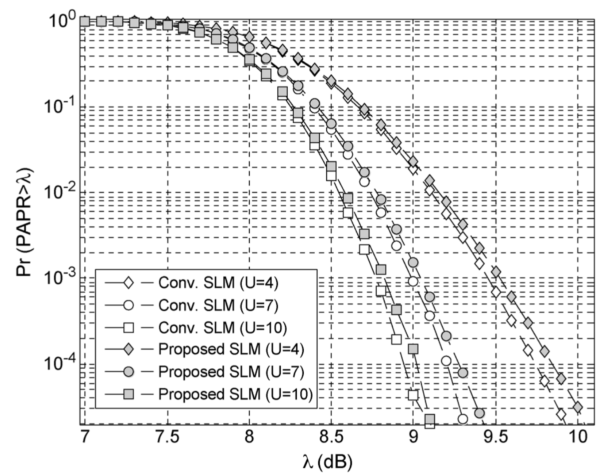

(a)

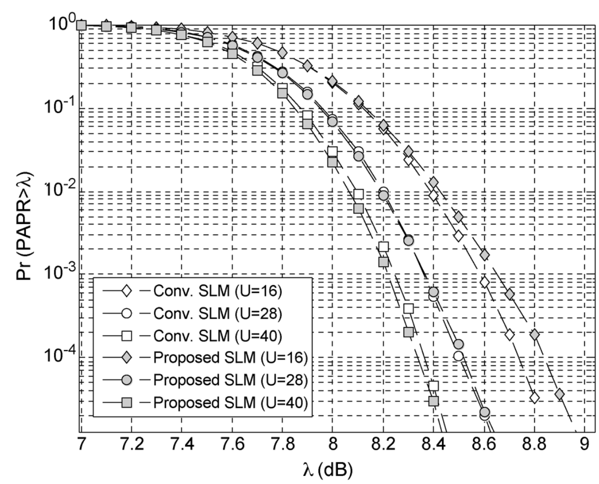

(b)

Fig. 4. Comparison of PAPR reduction performance of the conventional SLM and the proposed SLM schemes for $N = 512$. (a) QPSK. (b) 16-QAM.

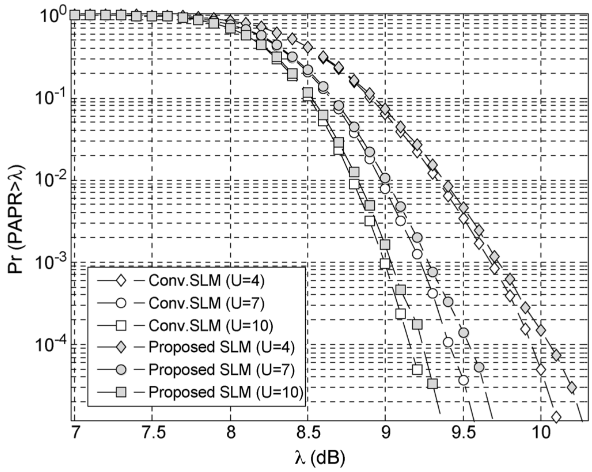

(a)

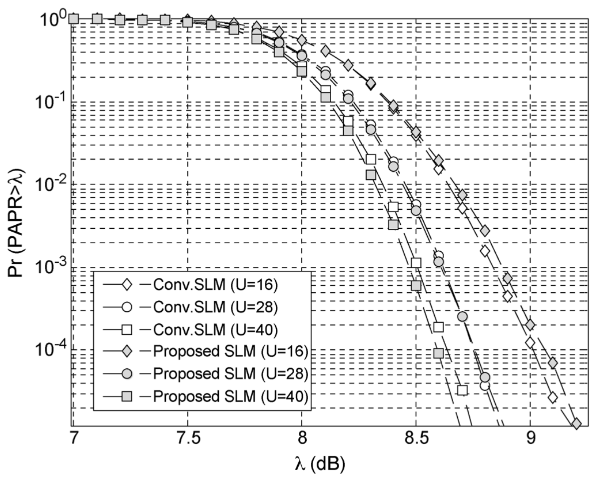

(b)

Fig. 5. Comparison of PAPR reduction performance of the conventional SLM and the proposed SLM schemes for Alamouti SFBC-OFDM with $N = 512$. (a) QPSK. (b) 16-QAM.

The CCDF for the Alamouti SFBC-OFDM in Fig. 5 also shows the similar PAPR reduction performance to the single-antenna OFDM case in Fig. 4.

Fig. 6 compares the BER performance of the proposed SLM scheme when two decoding schemes are used. The BER performance of Dec II is a little bit better than that of Dec I, which is almost identical to that of the original OFDM. Although the average power of $\mathbf{X}^{(\tilde{u})}$ in the proposed scheme is not shown in this paper, the average transmit power is reduced a little bit compared to the average symbol power of A_k, which is called a shaping gain. It is because the proposed SLM scheme generates $X_k^{(u)}$ by modifying the amplitude as well as the phase of A_k, which is explained in more detail in [21]. If the average transmit power of the proposed scheme is normalized to be the same as the average symbol power of A_k, the average transmit power increases as much as the shaping gain and consequently, the BER performance can be better than that of the original OFDM system. On the other hand, normalizing the transmit power increases the peak power as well and thus the PAPR reduction performance of the proposed SLM scheme becomes slightly worse than that of the conventional SLM scheme. Since it is not easy to implement power normalization in the practical system, the

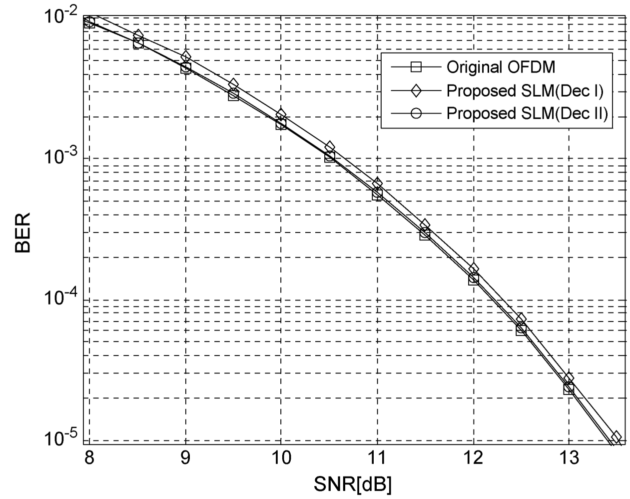

Fig. 6. Comparison of BER of the original OFDM and the proposed SLM scheme using Dec I and Dec II.

average power of the transmit symbol is considered to be the same as that of the input symbol in this paper.

VI. Conclusion

In this paper, a new low-complexity SLM scheme for the PAPR reduction of OFDM signals is proposed, which generates alternative signal sequences by simply adding mapping signal sequences to an OFDM signal sequence in the time domain. The proposed SLM scheme shows similar PAPR reduction performance as the conventional SLM scheme while reducing the computational complexity. Also, an SLM decoding scheme suitable for the proposed SLM scheme is proposed. This decoding method does not degrade the BER performance and also does not increase the computational complexity at the receiver compared to the conventional SLM scheme.

Although our work is focused on the single-antenna OFDM and the Alamouti SFBC-OFDM, the proposed SLM scheme can be applied to any kind of SFBC-OFDM systems if the input symbol sequence of one transmit antenna can be represented by linearly transforming the input symbol sequence of another transmit antenna.

References

[1] R. O'neal and L. N. Lopes, "Envelope variation and spectral splatter in clipped multicarrier signals," in *Proc. IEEE PIMRC*, Sep. 1995, pp. 71–75.

[2] T. Jiang, M. Guizani, H.-H. Chen, W. Xiang, and Y. Wu, "Derivation of PAPR distribution for OFDM wireless systems based on extreme value theory," *IEEE Trans. Wireless Commun.*, vol. 7, no. 4, pp. 1298–1305, Apr. 2008.

[3] T. Jiang and Y. Wu, "An overview: Peak-to-average power ratio reduction techniques for OFDM signals," *IEEE Trans. Broadcast.*, vol. 54, no. 2, pp. 257–268, Jun. 2008.

[4] D. Wulich and L. Goldfeld, "Reduction of peak factor in orthogonal multicarrier modulation by amplitude limiting and coding," *IEEE Trans. Commun.*, vol. 47, no. 1, pp. 18–21, Jan. 1999.

[5] X. B. Wang, T. T. Tjhung, and C. S. Ng, "Reduction of peak-to-average power ratio of OFDM system using a companding technique," *IEEE Trans. Broadcast.*, vol. 45, no. 3, pp. 303–307, Sep. 1999.

[6] T. Jiang, Y. Yang, and Y. Song, "Exponential companding transform for PAPR reduction in OFDM systems," *IEEE Trans. Broadcast.*, vol. 51, no. 2, pp. 244–248, Jun. 2005.

[7] T. Jiang, W. Xiang, P. C. Richardson, D. Qu, and G. Zhu, "On the nonlinear companding transform for reduction in PAPR of MCM signals," *IEEE Trans. Wireless Commun.*, vol. 6, no. 6, pp. 2017–2021, Jun. 2007.

[8] S. A. Aburakhia, E. F. Badran, and D. A. E. Mohamed, "Linear companding transform for the reduction of peak-to-average power ratio of OFDM signals," *IEEE Trans. Broadcast.*, vol. 55, no. 1, pp. 155–160, Mar. 2009.

[9] J. Tellado and J. M. Cioffi*, Multicarrier Modulation With Low PAR, Application to DSL and Wireless.*. Norwell, MA: Kluwer Academic Publisher, 2000.

[10] B. S. Krongold and D. L. Jones, "PAR reduction in OFDM via active constellation extension," *IEEE Trans. Broadcast.*, vol. 49, no. 3, pp. 258–268, Sep. 2002.

[11] R. W. Bäuml, R. F. H. Fischer, and J. B. Huber, "Reducing the peak-to-average power ratio of multicarrier modulation by selected mapping," *Electron. Lett.*, vol. 32, no. 22, pp. 2056–2057, Oct. 1996.

[12] S. H. Müller, R. W. Bäuml, R. F. H. Fischer, and J. B. Huber, "OFDM with reduced peak-to-average power ratio by multiple signal representation," *Ann. Telecommun.*, vol. 52, no. 1-2, pp. 58–67, Feb. 1997.

[13] C.-L. Wang and Y. Ouyang, "Low-complexity selected mapping schemes for peak-to-average power ratio reduction in OFDM systems," *IEEE Trans. Signal Process.*, vol. 53, no. 12, pp. 4652–4660, Dec. 2005.

[14] C.-Y. Hsu and H.-H. Chao, "Novel SLM scheme with low-complexity for PAPR reduction in OFDM system," *IEICE Trans. Fundamentals.*, vol. E91-A, no. 7, pp. 1689–1696, Jul. 2008.

[15] D.-W. Lim, J.-S. No, C.-W. Lim, and H. Chung, "A new SLM OFDM scheme with low complexity for PAPR reduction," *IEEE Signal Process. Lett.*, vol. 12, no. 2, pp. 93–96, Feb. 2005.

[16] A. Ghassemi and T. A. Gulliver, "Partial selective mapping OFDM with low complexity IFFTs," *IEEE Comm. Lett.*, vol. 12, no. 1, pp. 4–6, Jan. 2008.

[17] S.-J. Heo, H.-S. Noh, J.-S. No, and D.-J. Shin, "A modified SLM scheme with low complexity for PAPR reduction of OFDM systems," *IEEE Trans. Broadcast.*, vol. 53, no. 4, pp. 804–808, Dec. 2007.

[18] C.-P. Li, S.-H. Wang, and C.-L. Wang, "Novel low-complexity SLM schemes for PAPR reduction in OFDM systems," *IEEE Trans. Signal Process.*, vol. 58, no. 5, pp. 2916–2921, May 2010.

[19] S.-H. Wang and C.-P. Li, "A low-complexity PAPR reduction scheme for SFBC MIMO-OFDM systems," *IEEE Signal Process. Lett.*, vol. 16, no. 11, pp. 941–944, Nov. 2009.

[20] K. F. Lee and D. B. Williams, "A space-frequency trasmitter diversity technique for OFDM systems," in *Proc. IEEE GLOBECOM'00*, Nov. 2000, pp. 1473–1477.

[21] H.-B. Jeon, K.-H. Kim, J.-S. No, and D.-J. Shin, "Bit-based SLM schemes for PAPR reduction in QAM modulated OFDM signals," *IEEE Trans. Broadcast.*, vol. 55, no. 3, pp. 679–685, Sep. 2009.

[22] H. V. Sorensen, D. L. Jones, M. T. Heideman, and C. S. Burrus, "Real-valued fast Fourier transform algorithms," *IEEE Trans. Acoust., Speech, Signal Process.*, vol. assp-35, no. 6, pp. 849–863, Jun. 1987.

[23] D.-W. Lim, S.-J. Heo, and J.-S. No, "On the phase sequence set of SLM OFDM scheme for a crest factor reduction," *IEEE Trans. Signal Process.*, vol. 54, no. 5, pp. 1931–1935, May 2006.

[24] G. T. Zhou and L. Peng, "Optimality condition for selected mapping in OFDM," *IEEE Trans. Signal Process.*, vol. 54, no. 8, pp. 3159–3165, Aug. 2006.

[25] J. Yang and K. Cheun, "Low complexity implementation of Alamouti space-time coded OFDM transmitters," *IEEE Comm. Lett.*, vol. 8, no. 4, pp. 229–231, Apr. 2004.

Hyun-Bae Jeon received the B.S. and M.S. degrees in electrical engineering from Yonsei University, Seoul, Korea, in 1999 and 2001, respectively, and the Ph.D. degree in electrical engineering from Seoul National University, Seoul, Korea, in 2011. He was a Research Engineer at Samsung Electronics from 2001 to 2007. He is now a Senior Engineer at Samsung Electronics. His research interests include OFDM, PAPR, signal processing, and wireless communication systems.

Jong-Seon No (S'86–M'88–SM'09) received the B.S. and M.S.E.E. degrees in electronics engineering from Seoul National University, Seoul, Korea, in 1981 and 1984, respectively, and the Ph.D. degree in electrical engineering from the University of Southern California, Los Angeles, in 1988. He was a Senior MTS at Hughes Network Systems from February 1988 to July 1990. He was also an Associate Professor in the Department of Electronic Engineering, Konkuk University, Seoul, Korea, from September 1990 to July 1999. He joined the Faculty of the Department of Electrical Engineering and Computer Science, Seoul National University, in August 1999, where he is currently a Professor. His area of research interests includes error-correcting codes, sequences, cryptography, space-times codes, LDPC codes, and wireless communication systems.

Dong-Joon Shin (S'96–M'99–SM'09) received the B.S. degree in electronics engineering from Seoul National University, Seoul, Korea, the M.S. degree in electrical engineering from Northwestern University, Evanston, IL, and the Ph.D. degree in Electrical Engineering from University of Southern California, Los Angeles. From 1999 to 2000, he was a Member of Technical Staff in Wireless Network Division and Satellite Network Division, Hughes Network Systems, MD, USA. Since September 2000, he has been an Associate Professor in the Department of Electronic Engineering at Hanyang University, Seoul, Korea. His current research interests include error correcting codes, sequences, and discrete mathematics.